

Micro-structured electrode arrays: Glow discharges in Ar and N₂ at atmospheric pressure using a variable radio frequency generator

Christian Schrader^{a,*}, Lutz Baars-Hibbe^a, Karl-Heinz Gericke^a,
Eduard Marinus van Veldhuizen^b, Nina Lucas^c, Philipp Sichler^c, Stephanus Büttgenbach^c

^a*Institut für Physikalische and Theoretische Chemie, Technische Universität Braunschweig, Hans-Sommer Str. 10, D-38106 Braunschweig, Germany*

^b*Department of Physics, Technische Universiteit Eindhoven, Den Dolech 2, 5612 AZ Eindhoven, The Netherlands*

^c*Institut für Mikrotechnik, TU Braunschweig, Alte Salzdahlumer Str. 20, D-38124 Braunschweig, Germany*

Abstract

Micro-structured electrode (MSE) arrays consist of an interlocked, comb-like, capacitive electrode system with gap widths in the μm range. Large-area uniform glow discharges up to atmospheric pressure were penetrated with our arrays. In order to ignite glow discharges at atmospheric pressure this approach is established next to using dielectric barrier arrays and plasma jets. Because of the industrial, scientific and medical (ISM) limitation of available radio frequencies the usual frequency for experiments is 13.56 MHz. Using a variable radio frequency generator more information about the frequency dependent breakdown mechanisms are gained. The electric parameters of the non-thermal plasma system are characterized by a special probe with an upper frequency detection limit of 60 MHz.
© 2006 Elsevier Ltd. All rights reserved.

Keywords: Micro-structured electrode arrays; Glow discharge; Atmospheric pressure; Radiofrequency; Paschen curves

1. Introduction

Non-thermal plasma processing at atmospheric pressure is the subject of growing interest due to the possible applications in plasma chemistry and excitation. There are many approaches published in the last 15 yr to overcome the problems to generate and sustain stable, uniform and homogeneous non-thermal atmospheric pressure plasmas.

Massines et al. [1], Okazaki et al. [2], Trunec et al. [3] and Kelly Wintenberg et al. [4] successfully generated atmospheric pressure glow discharges with a dielectric barrier array, and Park et al. [5] developed an atmospheric pressure plasma jet producing stable and homogenous plasma. There are two approaches based on the Paschen similarity law ($pd = \text{const.}$), which scale down the distance of the electrodes to the micrometre range in order to ignite glow discharges at atmospheric pressure at moderate voltages working in the Paschen minima of the different gases. Stark and Schoenbach [6], Penache et al. [7] and

Eden et al. [8] use a micro-hollow-cathode array. We introduced micro-structured electrode arrays (MSE) consisting of an interlocked comb like electrode system with gap widths in the micrometre range [9–12]. The electrodes are arranged on an insulating substrate and are manufactured by means of modern micro-machining and galvanic techniques.

With the MSE array, it is possible to decompose perfluorocompounds (PFCs) [13]. CF₄ in particular is extensively used for semiconductor manufacturing processes, and as an exhaust gas of the processing tools it has proven to be particularly difficult to destroy and remove [14].

Another application of the MSE plasma source is the synergetic, successful concept of sterilisation and coating of food packaging materials. The reactive plasma species cause the physical destruction of the spores' cell walls, and induce the deposition of thin films as diffusion barrier resulting in packaging materials refinement. In our sterilisation experiments the thermo resistant spores of the vegetative bacteria *Bacillus cereus* (*B. cereus*) and the UV resistant spores of the fungus *Aspergillus niger* (*A. niger*) were deactivated.

*Corresponding author. Tel.: +49 531 391 5345; fax: +49 531 391 5396.
E-mail address: Ch.Schrader@tu-bs.de (C. Schrader).

This publication presents a new step of realising a homogeneous atmospheric pressure plasma source with very low breakdown and burning voltages in nitrogen, oxygen and air, respectively. We show in argon and nitrogen at atmospheric pressure that we can control the breakdown mechanism and accordingly the breakdown voltages by varying the frequency up to 55 MHz.

2. Experimental

Fig. 1 shows an MSE array and the electrode gap design supporting the ignition of the plasma. The design and production of the MSE arrays is already published in Ref. [13]. The characteristic MSE dimensions are electrode width (1350 μm), electrode thickness (100 μm) and electrode gap width (70 μm) in order to achieve high pressure ranges. The experimental set-up in Fig. 2 illustrates how the measurements with the special probe (ENI VI-Probe) with an upper frequency detection limit of 60 MHz have been carried out. The RF generator (Agilent 33250A 80 MHz connected to Amplifier Research Model 75AP250 75 W 5–250 MHz) is connected to the VI-Probe via a matching network (ENI MW-5D). A gas mixing unit supplies the vacuum chamber with different types of gases and the pressure control system adjusts the desired pressure.

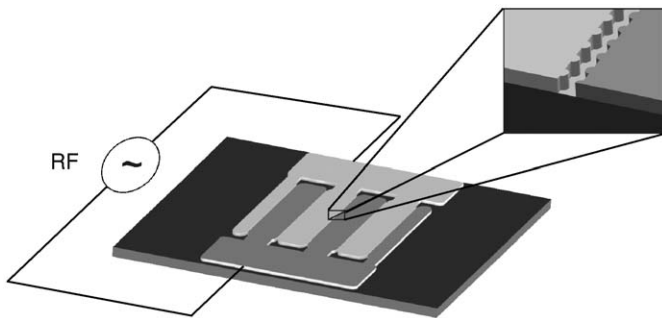


Fig. 1. Scheme of a micro-structured electrode (MSE) array.

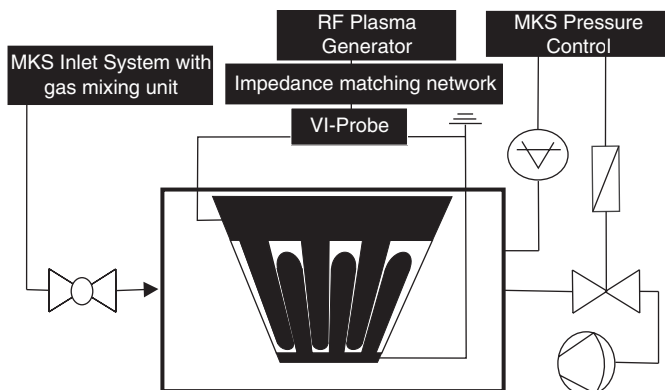


Fig. 2. Scheme of the experimental set-up.

3. Characterisation of the RF plasma

Due to the very small electrode gap width we can describe the behavior of the charged particles in the RF field of our system with the DC Townsend breakdown theory, depending on the pressure range and gas type. In order to explain the observed breakdown behavior Figs. 3 and 4 show the oscillation amplitudes z_0 of the Ar and N₂ ions calculated with the measured electric field strength E_0 using equation

$$z_0 = \frac{eE_0}{m\omega \sqrt{\omega^2 + \nu_C^2}} \quad (1)$$

in which E_0 is the field amplitude, m the mass of the charged particle, ω the angular frequency and ν_C the

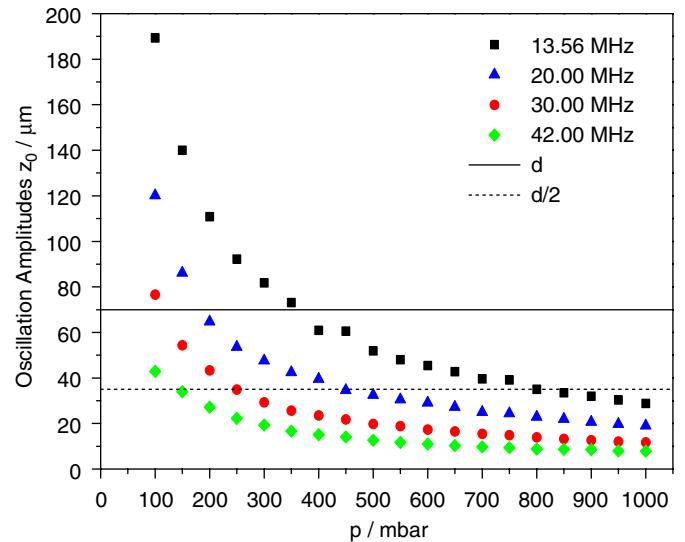


Fig. 3. Ar ion oscillation amplitudes for $d = 70 \mu\text{m}$ calculated with the measured electric field strength.

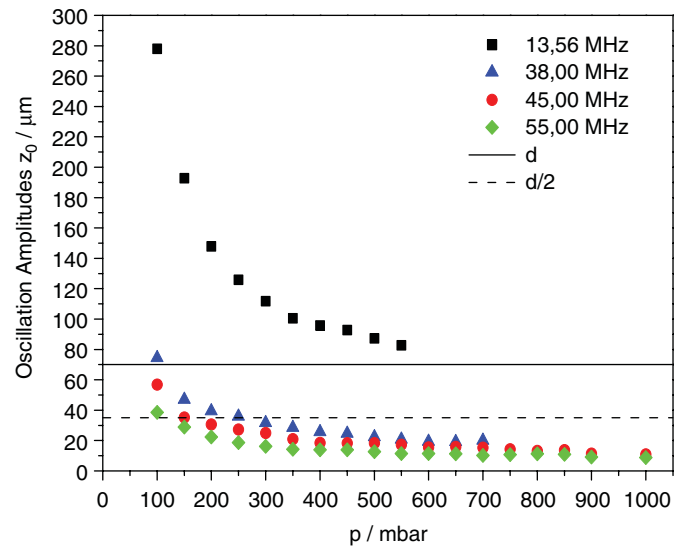


Fig. 4. N₂ ion oscillation amplitudes for $d = 70 \mu\text{m}$ calculated with the measured electric field strength.

ion-neutral collision frequency. This equation gives the extreme values derived from the solution (3) of the equation of motion (2) including the pressure dependent Lorentz collisional term in order to account for friction [15]:

$$m \frac{d^2 z}{dt^2} + m v_C \frac{dz}{dt} = e E_0 \sin \omega t, \quad (2)$$

$$z = -\frac{e E_0 v_C}{m \omega (\omega^2 + v_C^2)} \cos(\omega t) - \frac{e E_0}{m(\omega^2 + v_C^2)} \sin(\omega t). \quad (3)$$

The motion of the charged particles is drift controlled analogously to DC discharges, because the amplitudes of the electrons as well as the ions exceed $d/2$ ($35 \mu\text{m}$) [16]. The experimental Paschen curves measured in argon and nitrogen are illustrated in Figs. 5 and 6 including the Paschen formula fit [17,18] derived from the DC Townsend breakdown theory:

$$U_{\text{IP}} = \frac{B(pd)}{C + \ln(pd)}, \quad (4)$$

with

$$C = \ln \frac{A}{\ln((1/\gamma) + 1)}. \quad (5)$$

The minima of the fitted curves exhibit the minimal ignition voltage or energy, respectively. The maximum of Eq. (6)

$$\alpha = A p e^{-(Bp/E)}, \quad (6)$$

$$\left(\frac{E}{p}\right)_m = \left(\frac{U_{\text{IP}}}{pd}\right)_m = B, \quad (7)$$

corresponds to the minimal required energy specified in Eq. (7). The constant B (V/mbar cm), also known in this context as Stoljetow constant, is connected with the constant C from Eqs. (4) and (5) regarding the secondary

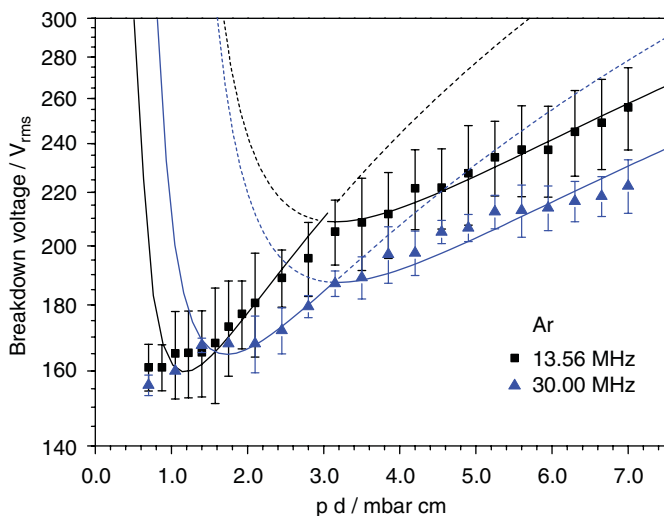


Fig. 5. Fitted Paschen curves in Ar. Comparison of the breakdown voltages of the different frequencies. The standard deviation describes the margin of deviation between three manufactured MSE samples.

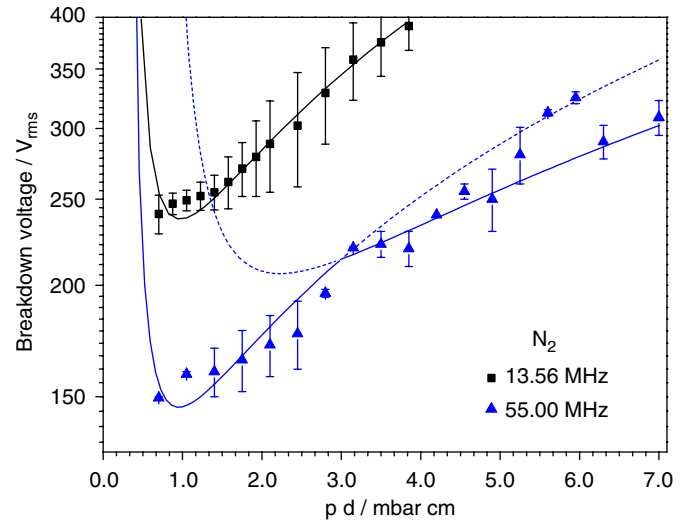


Fig. 6. Fitted Paschen curves in N_2 . Comparison of the breakdown voltages of the different frequencies. The standard deviation describes again the margin of deviation between three manufactured MSE samples.

electron amplification [19]. The experimental secondary electron emission coefficients γ are calculated using Eq. (5) with $A = 9.0 \text{ mbar}^{-1} \text{ cm}^{-1}$ [17]. The experimental curves in Fig. 5 and also in Fig. 6 are fitted twice where the transition from the DC Townsend regime or γ -regime to the high-frequency regime or α -regime is justified by the $d/2$ -criteria. The fitted constants B and C for the experiment in argon are listed in Table 1. For 13.56 MHz, the dominant breakdown mechanism changes from the DC Townsend mechanism (135.6 V/mbar cm , γ -regime) at low pressures to the high frequency regime (66.2 V/mbar cm , α -regime) at high pressures [21]. The B values of the RF experiments determined for $d = 70 \mu\text{m}$ are lower than the B values of the DC experiment [17] and decrease with increasing frequency. In the fit range at high pressures, where the high frequency mechanism already dominates at 13.56 MHz, the decrease of B with increasing frequency is not as strong as in the low pressure range. At low pressures, the dominating breakdown mechanism changes from the DC Townsend regime to the high frequency regime with increasing frequency. This interpretation is confirmed by Fig. 3: with increasing frequency the upper pressure limit fulfilling the $d/2$ criteria for the dominating DC Townsend regime ($z_0 > d/2$) is lowered, the high frequency regime becomes more dominant.

The experimental γ values confirm the present results. With the transition of the breakdown mechanism at low pressures from 13.56 to 30 MHz, the breakdown voltages increase slightly as shown in Fig. 4 at low pd values. The decreasing B value cannot compensate the strong decrease of the secondary electron emission coefficient γ (see Table 1) [21].

The fitted constants B and C for the experiment in nitrogen are also listed in Table 1. The B values of the RF experiments for $d = 70 \mu\text{m}$ are again lower than the B

Table 1

Fitted Ar and N₂ constants of the Paschen formula derived from Fig. 5 (*B* in V/mbarcm) as well as the secondary electron emission coefficients γ calculated using Eq. (5)

Frequency	<i>B</i> [Ar]	<i>C</i> [Ar]	γ [Ar]	<i>E/p</i> [Ar]	Regime [Ar]
DC	135 [17]	+0.97	3.4×10^{-2} [20]	75–450	γ
13.56 MHz	66.2 ± 1.4	-0.15 ± 0.03	2.88×10^{-5}	37–70	γ - α Transition
	135.6 ± 4.1	$+0.84 \pm 0.04$	2.10×10^{-2}	70–184	γ
20.00 MHz	63.8 ± 2.4	-0.16 ± 0.05	2.52×10^{-5}	34–72	γ - α Transition
	126.2 ± 2.3	$+0.73 \pm 0.03$	1.31×10^{-2}	72–118	γ
30.00 MHz	58.9 ± 2.2	-0.16 ± 0.05	2.52×10^{-5}	32–64	γ - α Transition
	95.4 ± 2.4	$+0.45 \pm 0.03$	3.18×10^{-3}	64–120	γ
42.00 MHz	55.5 ± 0.9	-0.10 ± 0.02	4.67×10^{-5}	30–58	γ - α Transition
	89.0 ± 3.7	$+0.48 \pm 0.05$	3.77×10^{-3}	58–107	γ
Frequency	<i>B</i> [N ₂]	<i>C</i> [N ₂]	γ [N ₂]	<i>E/p</i> [N ₂]	Regime [N ₂]
DC	256 [17]	+1.04	4.3×10^{-2}	75–450	γ
13.56 MHz	244.8 ± 4.1	$+1.03 \pm 0.02$	4.2×10^{-2}	102–344	γ
40.00 MHz	129 ± 19	$+0.48 \pm 0.26$	3.8×10^{-3}	66–94	γ - α Transition
	187.6 ± 4.7	$+1.06 \pm 0.03$	4.6×10^{-2}	103–265	γ
47.00 MHz	128.4 ± 6.5	$+0.69 \pm 0.10$	1.1×10^{-2}	57–92	γ - α Transition
	164.1 ± 6.1	$+1.12 \pm 0.04$	5.6×10^{-2}	100–218	γ
49.00 MHz	124 ± 33	$+0.65 \pm 0.56$	9.2×10^{-3}	58–77	γ - α Transition
	152.0 ± 6.7	$+1.05 \pm 0.05$	4.5×10^{-2}	85–219	γ
55.00 MHz	93 ± 12	$+0.20 \pm 0.21$	6.3×10^{-4}	51–70	γ - α Transition
	153 ± 12	$+1.05 \pm 0.08$	4.5×10^{-2}	82–214	γ

values of the DC experiment and decrease with increasing frequency with almost the same slope.

4. Ignition voltages dependent on applied radio frequencies

As already shown in Section 3 and demonstrated in He by Park et al. [5], the breakdown voltages are dependent on the applied radio frequency. After the characterisation of our plasma source, we are able to predict that with the high frequency regime starting to influence the breakdown mechanism at atmospheric pressure in argon and nitrogen the breakdown voltage decreases with increasing frequency as illustrated in Fig. 7. In nitrogen the decrease of the breakdown voltage with increasing frequency was measured at different pressures. In Fig. 8 a further similarity law like the Paschen law can be assumed. The breakdown voltage around 60.00 MHz seems to have the same amount like the breakdown voltage at half pressure with an applied radio frequency of 30.00 MHz. This correlation could justify the experimental obtained Eq. (8) :

$$U_{IP} = p\omega^{-1} = \text{const.} \quad (8)$$

5. Conclusion

This paper demonstrates a new promising path how the MSE arrays can be developed from a Paschen law

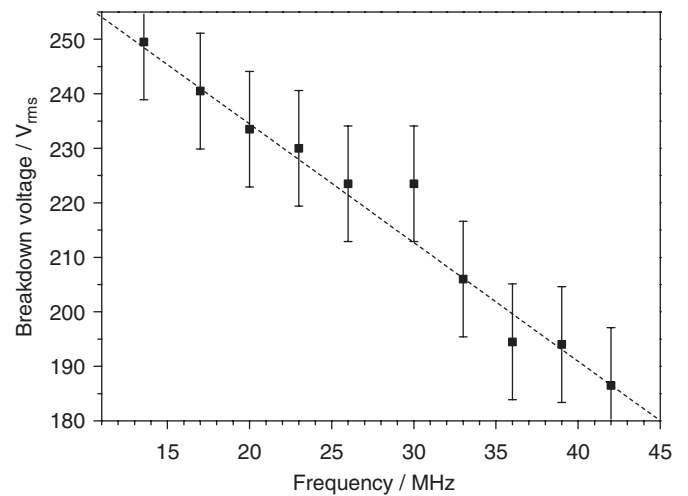


Fig. 7. Dependency of the experimental breakdown voltages on the applied frequency in 1000 mbar Ar.

optimized plasma source to an atmospheric pressure plasma application in several gases with discharge regime consideration. With variable RF frequencies it is possible to increase the working range and to improve the homogeneity of the plasma. Figs. 7 and 8 demonstrate that higher frequencies should result in further improvement of the plasma generation process. With very high frequencies (more than 100 MHz) the high frequency

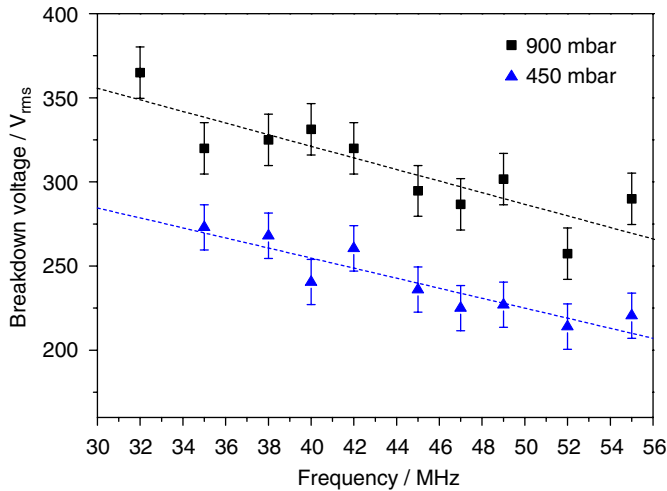


Fig. 8. Dependency of the experimental breakdown voltages on the applied frequency in N_2 .

regime should dominate the breakdown mechanism, even in air and with a very small electrode distance (less than $10\ \mu\text{m}$). This combination simultaneously results in lower breakdown voltages at high pressures and slows down the ageing of the MSE array, because the disadvantage of a dc discharge-sputtering-is completely avoided.

References

- [1] Massines F, Rabehi A, Decomps P, Ben Gadri R, Ségur P, Mayoux C. *J Appl Phys* 1998;83:2950–7.
- [2] Okazaki S, Kogoma M, Uehara M, Kimura Y. *J Phys D: Appl Phys* 1993;26:889–92.

- [3] Trunec D, Brablec A, Buchte J. *J Phys D: Appl Phys* 2001;34:1697–9.
- [4] Kelly Wintenberg K, Hodge A, Montie TC, Deleanu L, Shermann D, Reece Roth J, et al. *J Vac Sci Technol* 1999;17:1539–44.
- [5] Park J, Henins I, Hermann HW, Selwyn GS. *J Appl Phys* 2001;89:15–9.
- [6] Stark RH, Schoenbach KH. *J Appl Phys* 1999;85:2075–80.
- [7] Penache C, Bräuning-Demian A, Spielberger L, Schmidt-Böcking H. In: *Proceedings of the seventh international symposium on high pressure low temperature plasma chemistry (HAKONE VII)*; 2000. p. 501–5.
- [8] Eden JG, Park S-J, Ostrom NP, McCain ST, Wagner CJ, Vojak BA, et al. *J Phys D: Appl Phys* 2003;36:2869–77.
- [9] Geßner C, Scheffler P, Gericke K-H. In: *Proceedings of the seventh international symposium on high pressure low temperature plasma chemistry (HAKONE VII)*; 2000. p. 112–6.
- [10] Geßner C, Scheffler P, Gericke K-H. In: *Proceedings of the international conference on phenomena in ionized gases (XXV ICIPIG)*, vol. 4; 2001. p. 151–2.
- [11] Schlemm H, Roth D. *Surf Coat Technol* 2001;142–144:272–6.
- [12] Gericke K-H, Geßner C, Scheffler P. *Vacuum* 2002;65:291–7.
- [13] Baars-Hibbe L, Sichler P, Schrader C, Geßner C, Gericke K-H, Büttgenbach S. *Surf Coat Technol* 2003;174–175:519–23.
- [14] Harz C, Bevan JW, Jackson MW, Wofford BA. *Environ Sci Technol* 1998;32:682–7.
- [15] Reece Roth J. *Industrial plasma engineering*. Bristol, Philadelphia: IOP Publishing; 1995. p. 418–9.
- [16] Wiesemann K. *Einführung in die Gaselektronik*. Stuttgart: B.G. Teubner; 1976. p. 267–8.
- [17] Raizer YuP. *Gas discharge physics*, vol. 56. Berlin, Heidelberg: Springer; 1997. p. 133–5.
- [18] Grill A. *Cold Plasma in materials fabrication*. New York: IEEE Press; 1994. p. 24–34.
- [19] Baars-Hibbe L, Sichler P, Schrader C, Lucas N, Gericke K-H, Büttgenbach S. *J Phys D: Appl Phys* 2005;38:510–7.
- [20] Brown SC. *Basic data of plasma physics*. Cambridge: M.I.T. Press; 1966. p. 219–35.
- [21] Baars-Hibbe L, Sichler P, Schrader C, Gericke K-H, Büttgenbach S. *Plasma Process Polym* 2005;2:174–82.